

# Challenges and Progress in the Development of High-Temperature Shape Memory Alloys Based on NiTiX Compositions for High-Force Actuator Applications

*Santo Padula II, Glen Bigelow, Ronald Noebe, Darrell Gaydos, and Anita Garg  
NASA Glenn Research Center, 21000 Brookpark Rd., Cleveland, OH 44135*

## Abstract

Interest in high-temperature shape memory alloys (HTSMA) has been growing in the aerospace, automotive, process control, and energy industries. However, actual materials development has seriously lagged component design, with current commercial NiTi alloys severely limited in their temperature capability. Additions of Pd, Pt, Au, Hf, and Zr at levels greater than 10 at.% have been shown to increase the transformation temperature of NiTi alloys, but with few exceptions, the shape memory behavior (strain recovery) of these NiTiX systems has been determined only under stress free conditions. Given the limited amount of basic mechanical test data and general lack of information regarding the work attributes of these materials, a program to investigate the mechanical behavior of potential HTSMAs, with transformation temperatures between 100 and 500 °C, was initiated. This paper summarizes the results of studies, focusing on both the practical temperature limitations for ternary TiNiPd and TiNiPt systems based on the work output of these alloys and the ability of these alloys to undergo repeated thermal cycling under load without significant permanent deformation or “walking”. These issues are ultimately controlled by the detwinning stress of the martensite and resistance to dislocation slip of the individual martensite and austenite phases. Finally, general rules that govern the development of useful, high work output, next-generation HTSMA materials, based on the lessons learned in this work, will be provided.

## Introduction

In recent years, the desire to develop compact energy efficient actuation schemes and morphing structures has dictated the investigation of a number of systems including shape memory alloys, structured bi-metallics, and piezoelectric materials. Due to the ever increasing demand to obtain both passive and active control capability in systems where high forces resist the actuation event, shape memory alloys (SMA) have slowly worked their way to the forefront as the most viable choice.

The shape memory effect, which was originally observed in the binary NiTi system, is caused by a reversible change in crystal structure which occurs when the material is heated and cooled through a transformation cycle. Below the transformation temperature, the material is martensitic and deforms predominately via twinning mechanisms, although

slip becomes dominant at higher stress levels. Above the transformation temperature, austenite becomes the stable phase. This phase only deforms via slip processes and therefore any strain that is accommodated by the austenite is not reversible. It is the ability of these materials to undergo reversible deformation that makes them good candidates for actuator systems.

The most viable shape memory alloys have been based on binary NiTi, but this class of SMA has a very low temperature capability, in the range of -100 to 90 °C. Many of the envisioned actuator applications require temperature capability far in excess of this level. For instance, aeronautics and aerospace propulsion technologies could substantially benefit from SMA actuation systems, but these technologies require alloys with transformation temperatures in the 200-1000 °C range. Similarly, automotive applications in and around the engine would require alloys with at least 100-300 °C capability. As a result, work was undertaken to investigate ternary systems based on the binary NiTi composition in the hopes to develop higher transition temperature alloys. Various alloying additions including Pd, Pt, Au, Hf, and Zr have been shown to increase the transformation temperatures to various degrees with upper limits approaching 1050 °C for TiPt alloys [1,2,3,4]. Albeit, some of these alloying levels, would seem to make the materials unattainable due to cost considerations (i.e., alloys containing 30-50 at% Pt would be prohibitively expensive). Still these systems have the potential to replace extremely heavy hydraulic and pneumatic systems with a compact, lightweight, solid-state component, which in some applications could balance the initial high costs of the materials.

However, the mere exhibition of shape memory behavior at elevated temperature is not sufficient when considering these materials for actuator applications. To date, much of the published literature has demonstrated or investigated the high-temperature shape memory behavior of these materials under stress free conditions [5,6,7,8,9]. In real applications, the material not only has to exhibit the shape memory effect at high temperatures but must also be able to perform work against an externally applied load in order to function properly. In some cases, the increases in transformation temperature, which occur as a result of alloying, come at the expense of a seriously diminished work capability [10,11].

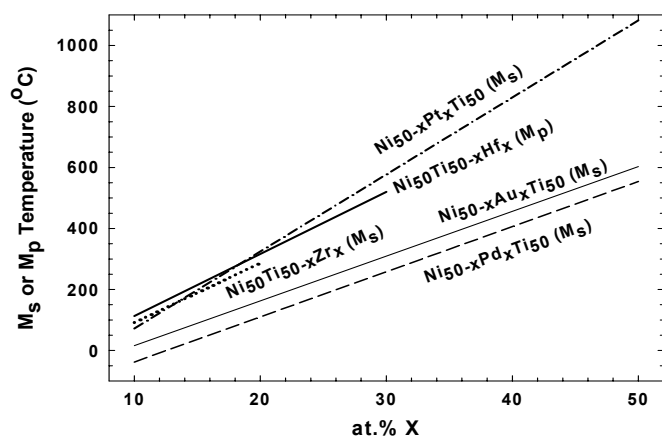


Figure 1: Effect of alloy content on the transformation temperature of various ternary SMA systems.

However, useful work characteristics have been verified in TiNiHf thin films [12,13] and bulk TiNiPt [10] and TiNiPd [14] alloys. Therefore, the possibility of developing high-temperature shape memory alloys, specifically for high-force actuator type applications, seems plausible today.

As will be demonstrated, the inability of some high-temperature alloys to generate meaningful work is the direct result of changes in the mechanical properties brought about by the alloying coupled with the temperature range where the material is expected to operate. Thus, even though a material may exhibit shape memory behavior with a high transition temperature, the alloy may not necessarily be useful from an actuator perspective due to the underlying behavior of the material in the presence of an external stress. Consequently, many factors must be taken into account in determining if a candidate material will be suitable for actuator applications: the foremost being the work characteristics of the alloy.

## Materials & Procedures

### Material Processing and Characterization

Ternary alloys based on binary NiTi with additions of Pt and Pd were chosen based on previous work that showed transformation temperatures between room temperature and 1050 °C were possible [1,15,16]. In this work, ternary alloying additions of 15-46 at% Pd or Pt were utilized, with the addition being substituted primarily for nickel. HTSMA ingots were made via vacuum induction melting (VIM). The process consisted of creating melts in a graphite crucible using high purity elemental constituents and subsequently casting into a 25.4 mm diameter by 102 mm long copper mold outfitted with a hot top section sized appropriately to feed the casting during solidification. These ingots were subsequently heat treated in a vacuum furnace at 1050 °C for 72 hours in order to homogenize the microstructure. After heat treatment, the ingots were placed into mild steel cans, evacuated, sealed and extruded at 900-1200 °C using a 7:1 area reduction ratio.

Cylindrical dog-bone tensile samples measuring 50.80 mm were CNC machined from each of the extrusion rods. These

samples were outfitted with threaded grip ends and contained a gage section that was 17.4 mm long by 3.81 mm in diameter. Subsequent to the machining operation, the samples were given a stress relief heat treatment at 400 °C for 1 hour for Pd-containing alloys while the stress relief treatment for the Pt-containing alloys varied from 440 to 700 °C depending on composition.

The microstructures of the alloys were examined after the stress relief heat treatment using a combination of scanning electron microscopy (SEM) and transition electron microscopy (TEM). Standard metallographic mounts were used for SEM with electron dispersive spectroscopy (EDS) being employed to ascertain the basic microstructural components present. Hence, a rough estimate of the volume fraction and general composition of second phase particles was assessed. To conclusively identify the structure of any other phases present in the material, electron diffraction was performed during TEM analysis. TEM samples were prepared by electrical discharge machining of 3.81 mm diameter by 0.5 mm thick disks from the various materials. These disks were subsequently ground to a thickness of 0.15 mm, dimpled and ion milled to final electron transparency.

### Mechanical Testing

Mechanical testing was performed in a servo-hydraulic load frame (equipped with a digital controller) using hot grips and inductive heating. Strain measurements were made using a 12.7 mm gage length, high temperature extensometer equipped with 85 mm long quartz probes with a v-chisel edge. The extensometer had a maximum range of +20/-10% strain. All temperature measurements were made using type K thermocouples which were directly spot welded to the specimens. Temperature gradients along the gage section of the sample were maintained to within +/-0.5% of the test temperature.

Monotonic tension tests were conducted using strain control with the applied stress direction parallel to the extrusion direction. Tests were conducted at a rate of  $1 \times 10^{-4} \text{ sec}^{-1}$  with the tensile specimens run to failure or until the 20% strain limit of the extensometer was reached, in which case the samples were unloaded prior to fracture.

The work characteristics of the alloys were determined using constant load, strain recovery tests (referred to as load-bias tests). In this test, specimens were strained at room temperature to a desired load at a rate of  $1 \times 10^{-4} \text{ sec}^{-1}$ . Once the desired load was reached, the controller was switched to load control in order to maintain a constant load-bias. Specimens were then cycled twice from room temperature to approximately 100 °C above the austenite finish temperature with the strain recorded continuously. Heating rates were held at 10 °C/min. Once two cycles were completed, the specimen was unloaded at room temperature and subsequently strained until the next desired load bias was reached.

Table 1: Transition temperatures and work outputs as a function of composition.

Extrusion #	Composition (at.%)				Mf (°C)	Af (°C)	Max Work (J/cm <sup>3</sup> )	Ref
	Ti	Ni	Pd	Pt				
8	50	30		20	245	279	8.73	10
15	50	30		20	195	233	9.88	current study
17	50	30		20	221	257	10.47	current study
29	50.5	29.5		20	274	337	9.3	19
32	50.5	24.5		25	390	505	1.52	current study
7	50	20		30	534	615	0	10
19	50	20		30	524	597	0.1	10
36	50.5	34.5	15		65	83	8.64	11
37	50.5	29.5	20		123	143	8.24	11
38	50.5	24.5	25		178	197	9.06	11
24	50.5	19.5	30		233	259	9.22	11,14,17
48	50.5	19.5	25	5	228	259	8.86	11,17
50	50.5	3.5	46		469	513	0.00	11

At this point the thermal cycling process was repeated. The specific work output capability of the alloy was then determined by taking the product of the applied bias stress and the resulting strain recovered during the martensite-to-austenite transformation from the second heating cycle.

## Results

### Composition and Microstructure

All of the Pt and Pd containing alloys reviewed in this investigation were processed in our laboratories with aim compositions that were either stoichiometric (i.e., Ti:(Ni+X) = 50:50 at.%, where X is either Pt or Pd) or slightly Ti-rich with an aim Ti-content of 50.5 at.%. Some of the alloys have been described previously [10,11,14,17,19] while additional alloys represent more recent data, as indicated in Table 1. Chemical analysis by inductively coupled plasma spectroscopy indicated that all the materials were within experimental error of their aim composition, and contained several tenths of an atomic percent oxygen and carbon.

The resulting microstructures were similar in all cases, since the alloys were either near stoichiometric or slightly Ti-rich. They were essentially single phase, consisting of an orthorhombic B19 martensite when analyzed at room temperature and had a recrystallized equiaxed grain structure

of 10 to 50  $\mu\text{m}$  depending on the extrusion temperature. All the alloys also contained about 2-4 vol% total of additional phases. One was the intermetallic phase  $\text{Ti}_2(\text{Ni,Pt})$  or  $\text{Ti}_2(\text{Ni,Pd})$ , depending on the ternary addition, which is isostructural to  $\text{Ti}_2\text{Ni}$ . The other phase present was an FCC-structured Titanium carbide or oxy-carbide (e.g.,  $\text{TiC}$  or  $\text{Ti(C,O)}$ ). The intermetallic phase was usually several microns in size while the  $\text{Ti(C,O)}$  was less than 2  $\mu\text{m}$  with an average size of 0.5  $\mu\text{m}$ . Figure 2 shows representative microstructures from the TiNiPt and TiNiPd systems, respectively.

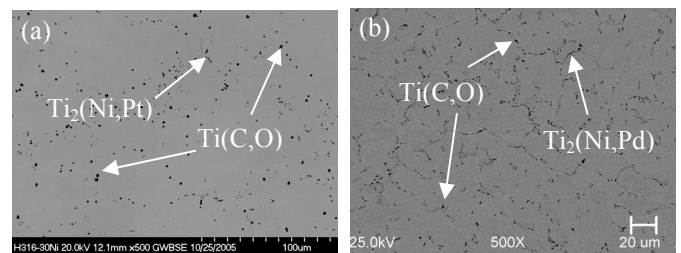


Figure 2: Microstructures of (a)  $\text{Ni}_{30}\text{Pt}_{20}\text{Ti}_{50}$  alloy ( $M_f=220^\circ\text{C}$ ,  $A_f=245^\circ\text{C}$ ) and (b)  $\text{Ni}_{19.5}\text{Pd}_{30}\text{Ti}_{50.5}$  alloy ( $M_f=233^\circ\text{C}$ ,  $A_f=250^\circ\text{C}$ ).

### Temperature Dependence of Work Output

Since a primary application for high-temperature shape memory alloys is for integration with adaptive structures or simply as solid state actuators, work output (or the ability of the material to recover strain against some biasing force) was considered the most important property for screening the viability of different alloys. Consequently, load-bias testing was performed to quantify the work output of each of the alloys. This data is summarized in Table 1 along with the full temperature range of the transformation ( $M_f$  to  $A_f$ ) for each alloy.

For the constant-load, strain-temperature tests, the load was applied to the sample at room temperature and then held constant as the sample was heated and cooled twice through the transformation regime. The work output as function of stress was then determined from the second heating and cooling cycle imposed at each load level. The load was then incremented to the next load level and the test repeated until the sample failed from tensile overload. The maximum work output was usually observed at stress levels between 350 and 450 MPa and is included in Table 1.

To determine the transformation temperatures for each alloy, the sample was heated through the transformation range under essentially zero load and the length change as a function of temperature was determined. In this way the transformation temperatures were determined directly on each tensile sample prior to starting the load bias test. From this data the full range of transformation ( $M_f$  to  $A_f$ ) was determined and included in Table 1.

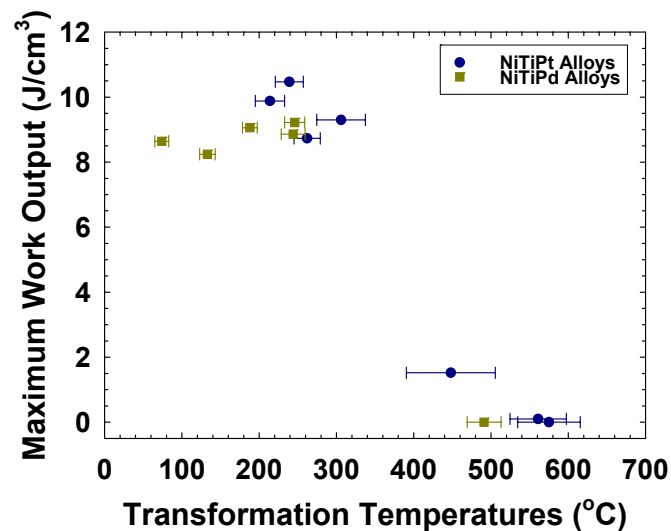


Figure 3: Work output as a function of the level of Pt and Pd content. Alloys containing ternary additions that produce transformation temperatures greater than about 300 °C show almost no usable work output.

To better summarize all this data, the maximum work output was plotted in Figure 3 as a function of the transformation range, so that the full range over which the transformation occurs ( $M_f$  to  $A_f$ ) for each alloy is clearly indicated. This provides much more information than plotting the work output

as a function of just a single transformation temperature like the  $M_s$ . From the figure, it is clear that very good and consistent work output of between 8 and 11 J/cm<sup>3</sup> is achieved for alloys with transformation temperatures between 100 and approximately 300 °C. However, for alloys with transformation temperatures above this range, the work output drops off almost catastrophically so that alloys with transformation temperatures in the neighborhood of 500 °C, are capable of essentially zero work output. This was the case for both the Pd and Pt containing alloys. Consequently, in order to better understand this phenomenon, a detailed investigation of the work behavior and monotonic tensile characteristics of specific alloys that exhibited both reasonable and poor work output was conducted. The results of this investigation are presented in the following section.

### Monotonic and Load-Biased Mechanical Behavior of Select Alloys

The difference between alloys with reasonable work output and extremely poor performance could not be attributed to microstructural differences as all the materials investigated contained 2-4 vol% of essentially the same second phases. Furthermore, the volume fraction and size of these additional phases were such that they would not provide any advantage in terms of strengthening. Consequently, monotonic tension tests were performed at temperatures both above and below the transformation range for select alloys with reasonable and poor work output. Doing so provided important information regarding the relative strengths of each of the stable phases (martensite and austenite) in a given alloy.

In Pt containing alloys, the yield stress of the parent austenite phase was greater than that of the lower temperature martensite phase, for all additions up to 20 at% Pt. At 25 at% Pt levels, the monotonic strength of the austenite was greater than the martensite phase but not appreciably. Similarly for the NiTiPd alloys, the austenite strength was considerably higher than that of the low-temperature martensite phase for all alloys with additions up to 30 at% Pd. Conversely, for additions of Pt or Pd greater than the aforementioned levels, the opposite behavior was observed: the yield behavior of the martensite was greater than that of the parent austenite, with the strength of the parent austenite decreasing dramatically with further increases in temperature above the  $A_f$ .

Figures 4-7 show the differences in observed monotonic deformation response, for select alloys, at temperatures where the martensite (M) and austenite (A) phases were stable. These monotonic strengths, in part, dictated the observed load-biased strain recovery responses of the alloys. For all alloy compositions up to 20 at% Pt and 30 at% Pd, respectively, reasonable work output characteristics were observed (See Figures 8 and 9). These good work characteristics resulted because the strength of the parent austenite was greater than that of the low temperature martensite, as shown in Figures 4 and 5 for the Pt and Pd alloys, respectively.

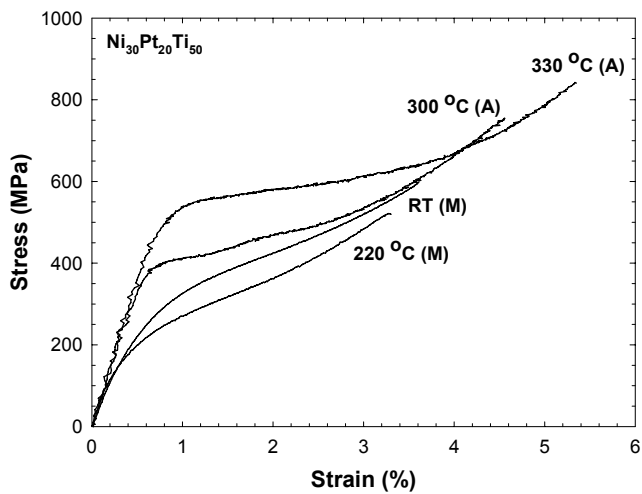


Figure 4: Monotonic Stress-Strain Response of  $Ni_{30}Pt_{20}Ti_{50}$  alloy ( $M_f=220\text{ }^\circ\text{C}$ ,  $A_f=245\text{ }^\circ\text{C}$ ).

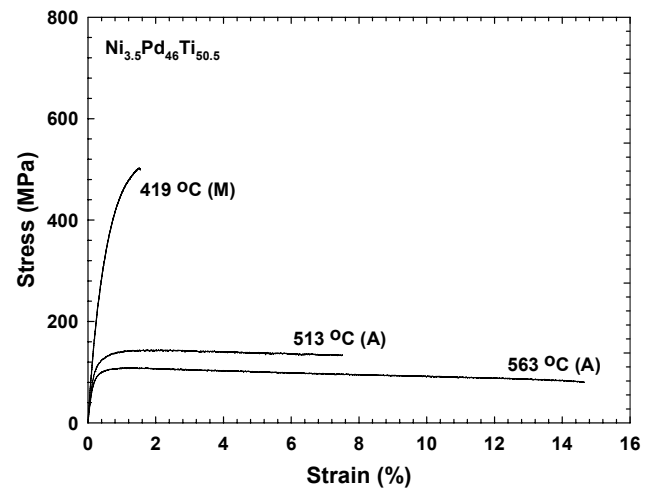


Figure 7: Monotonic Stress-Strain Response of  $Ni_{3.5}Pd_{46}Ti_{50.5}$  alloy ( $M_f=469\text{ }^\circ\text{C}$ ,  $A_f=513\text{ }^\circ\text{C}$ ).

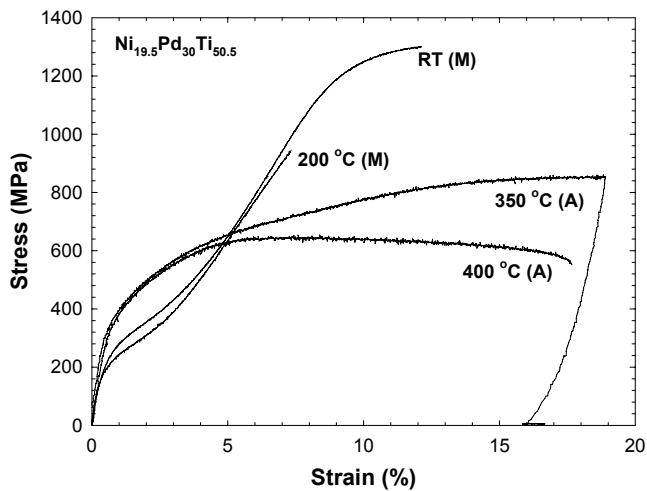


Figure 5: Monotonic Stress-Strain Response of  $Ni_{19.5}Pd_{30}Ti_{50.5}$  alloy ( $M_f=233\text{ }^\circ\text{C}$ ,  $A_f=250\text{ }^\circ\text{C}$ ).

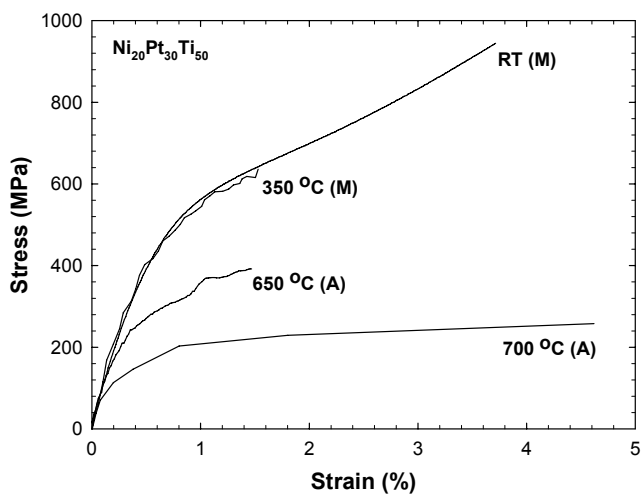


Figure 6: Monotonic Stress-Strain Response of  $Ni_{20}Pt_{30}Ti_{50}$  alloy ( $M_f=530\text{ }^\circ\text{C}$ ,  $A_f=600\text{ }^\circ\text{C}$ ).

This, then, allows large amounts of twin deformation to occur under the bias stress with minimal or no slip deformation resulting in the parent austenite once the material is heated through the transformation. As a result, good work characteristics were observed since the majority of the deformation processes involved are recoverable and not permanent.

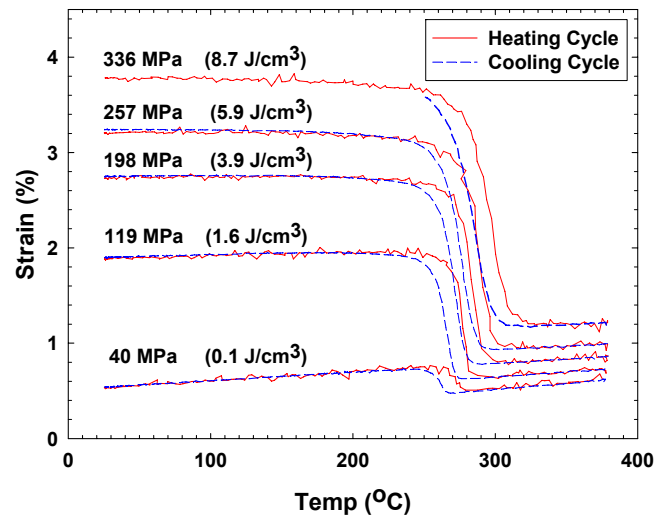


Figure 8: Work output characteristics of  $Ni_{30}Pt_{20}Ti_{50}$  alloy ( $M_f=220\text{ }^\circ\text{C}$ ,  $A_f=245\text{ }^\circ\text{C}$ ) at various bias stress levels.

The overall trend in strength of the austenite phase and martensite phase as a function of alloying content is best summarized in Figure 10. This figure shows the yield strength of the austenite phase determined at  $50\text{ }^\circ\text{C}$  above the  $A_f$  and the strength of the martensite phase determined at  $50\text{ }^\circ\text{C}$  below the  $M_f$  for each ternary TiNiPd alloy studied. The yield strength of the austenite decreased with increasing Pd content with a rapidly accelerating rate of decrease in yield strength at higher Pd levels.

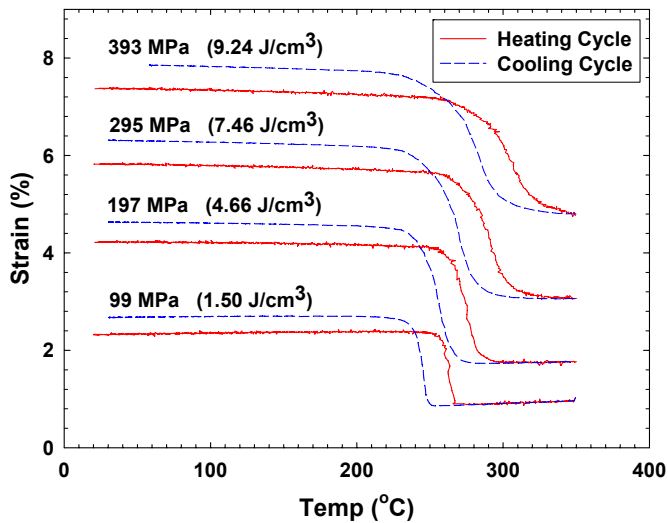


Figure 9: Work output characteristics of  $Ni_{19.5}Pd_{30}Ti_{50.5}$  alloy ( $M_f=233^\circ C$ ,  $A_f=250^\circ C$ ) at various bias stress levels.

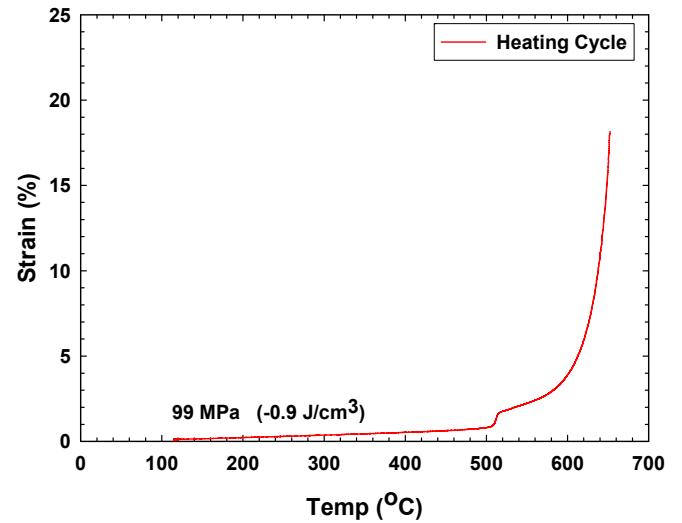


Figure 11: Work output characteristics of  $Ni_{3.5}Pd_{46}Ti_{50.5}$  alloy ( $M_f=469^\circ C$ ,  $A_f=513^\circ C$ ).

Conversely, as the Pd content increased the strength of the martensite phase (or the resistance to twinning/detwinning) increased; at an accelerating rate with increasing Pd content. Consequently, at lower Pd levels the austenite phase was stronger than the martensite phase and the alloy was capable of reasonable work output. At higher levels of Pd, the strengths of the phases begin to approach each other and actually inverted starting at about 37 at.% Pd.

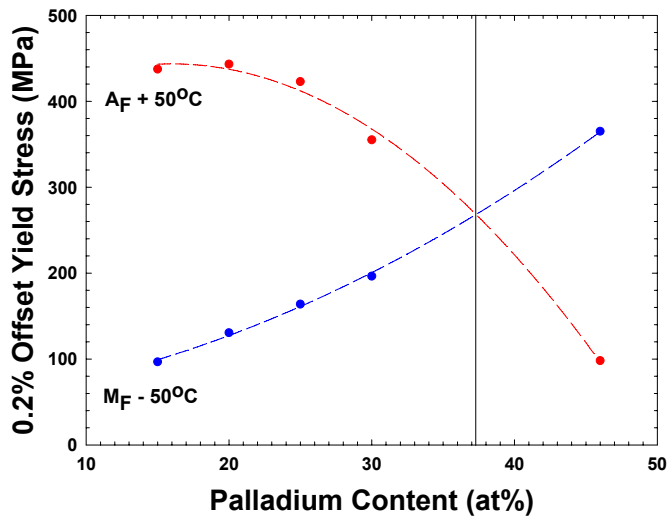


Figure 10: Effect of Pd content on the yield behavior of the martensite and austenite strengths.

Consequently, at Pd levels  $> 37$  at.%, any stress needed to detwin the martensite far exceeds the yield behavior of the austenite and therefore it would be difficult if not impossible to derive significant work out of these alloys. For example, in the case of the  $Ti_{50.5}Ni_{3.5}Pd_{46}$  alloy, the lowest bias-stress level attempted resulted in significant deformation and fracture of the alloy prior to reaching the cooling portion of the first cycle (Figure 11).

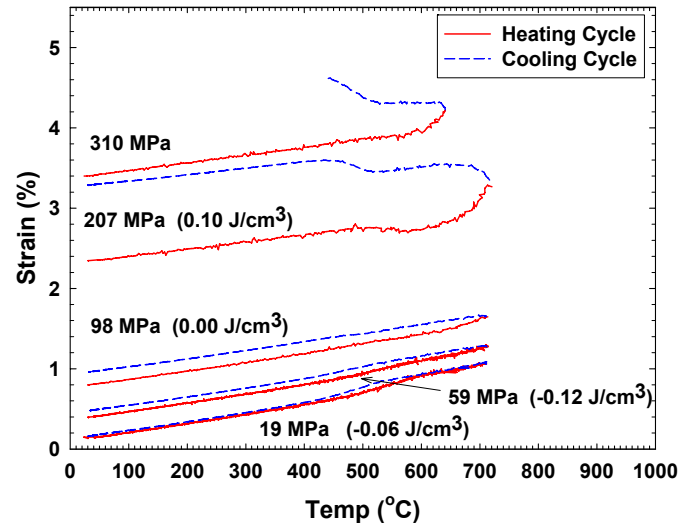


Figure 12: Work output characteristics of  $Ni_{20}Pt_{30}Ti_{50}$  alloy ( $M_f=530^\circ C$ ,  $A_f=600^\circ C$ ).

The TiNiPt alloys display similar behavior to the TiNiPd alloys shown in Figure 10, with the relative strength of the austenite and martensite inverting at Pt levels between 25 and 30 at.%. However, even at the highest level of Pt studied (30 at.%), the alloy did exhibit simple no-load shape memory behavior [10], but under bias stress conditions, no useful work output was observed (See Figure 12). The inability of the higher alloy content materials to produce work was the result of the relationship between the austenite and martensite strengths, as reported earlier. In the case of  $Ni_{20}Pt_{30}Ti_{50}$ , the strength of the martensite was substantially greater than that of the austenite. As such, the martensite is more resistant to detwinning than the austenite is to slip and no significant recoverable strain can be imparted to the material at low temperatures without permanently deforming the material upon transformation, since the austenite is susceptible to

permanent deformation at this same bias stress. This condition, then, sets up a scenario whereby the plastic deformation of the austenite swamps any recoverable strain that can be imparted to the martensite at low temperature, thereby producing poor load-biased work characteristics. Consequently, the ability of a material to exhibit shape memory behavior, by itself, is a poor indicator of how that material will perform under load-biased conditions and should not be used as a factor when trying to identify shape memory alloys with high force capability.

Even those alloys which exhibit reasonable work characteristics can have deleterious effects which can prohibit them from being used in real world applications. The “walking” or ratcheting that occurs during the cooling portion of each thermal cycle in Figure 9 would cause any device utilizing this material to be unstable and potentially unusable. As can be seen in Figure 9, no permanent deformation of the high temperature austenite was observed at any of the bias stress levels performed. Thus, the ratcheting which develops does so during the cooling portion of the cycle and can be related predominately to permanent deformation of the martensite. This means that both detwinning and slip processes are active in the martensite at the stress levels conducted herein. Hence, resistance to slip is not only important for the austenite but is equally important for the martensite if good work characteristics are desired. To this end, various means of developing the correct mechanical characteristics will subsequently be presented.

## Discussion

It is now clear that the catastrophic decrease in work capability for TiNiPd and TiNiPt alloys with transformation temperatures above 300 °C, (shown in Figure 3), has its origin in the various strength levels of the austenite and martensite phases and their relationship to each other. For both alloys the yield strength of the austenite phase begins to drop off precipitously at temperatures above 300 °C while the strength of the martensite phase continues to increase with increasing alloy content. Consequently, at the higher alloying levels studied, the strength of the martensite phase approaches that of the parent austenite. As this happens there is a lower resistance of the austenite phase to slip deformation which in turn lowers the ability of the material to produce significant work output. Since the parent austenite can no longer resist deformation at higher stresses and the low temperature martensite is more resistant to deformation by detwinning, less load can be applied to the material, subsequently reducing the amount of strain that can be imparted to the martensite phase. This translates into lower strain recovery at a lower bias-stress during the transformation and therefore less work capability. In the limiting case, where the strengths of the two phases completely invert, the amount of plastic deformation that results leads to a level of permanent deformation that swamps the recoverable strain component, thereby producing negative work. This, of course, is not desirable but does demonstrate the deleterious effects that an improper balance in properties

between the martensite and austenite phases can have on SMA performance and illustrates one of the primary challenges in developing viable high-temperature shape memory alloys.

Although the lower alloying levels did result in materials with promising work levels for actuator applications, in some cases another deleterious effect, (e.g., ratcheting) was observed. This effect warrants further attention and study since viable actuator systems can only be developed upon successful mitigation of this performance robbing effect, which also has its roots in the plastic (non-recoverable) deformation of the shape memory alloy. While in some cases ratcheting can be due to overheating of the alloy during thermal cycling resulting in a component of plastic deformation of the austenite with each cycle [14], under more normal operating conditions it is due to plastic deformation of the martensite (as shown in Fig. 9). In this case, the stress at which slip begins in the martensite is close to the stress for twinning/detwinning and therefore an amount of plastic deformation occurs with each load-biased thermal cycle.

## Factors Important for Good Work Output

As previously discussed, the mere exhibition of shape memory effect is not sufficient to determine whether an alloy has a useful balance of properties for actuator applications. Therefore screening for viable high-temperature shape memory alloys requires load-bias testing or sufficient monotonic tensile testing on both sides of the martensite-to-austenite phase transformation to determine whether the alloys have the appropriate balance of properties.

In designing alloys for high-temperature use, it is clear that there are some underlying characteristics that must be present for an alloy to exhibit reasonable work output with good dimensional stability at elevated temperature. Since the resulting work output of the material is directly tied to the amount of recoverable strain energy that can be stored in the system, optimizing the material, such that the martensite not only has a low stress for deformation by detwinning but also has a high resistance to dislocation slip, is imperative. However, the aforementioned characteristics must also be accompanied by an austenite phase which is highly resistant to slip with the difference in yield strength between the martensite and austenite phases being as large as possible. At the same time, this improvement in resistance to slip cannot occur at the significant expense of ductility or toughness of the alloy. Therefore, development of viable high-temperature shape memory alloys is a balancing act between various properties.

## Methods for Improving Material Performance

In the past, several studies have focused on improving the no-load shape memory behavior of NiTiPd alloys through various mechanisms aimed at enhancing the alloys resistance to slip and thus promoting greater deformation by twin motion in hopes of enhancing the stress-free shape memory behavior of these alloys. Such studies have involved the use of solid solution strengthening [5,6], precipitate strengthening [7], and various thermomechanical processing routines [8,9], with little success in the former and moderate success with the other

approaches. In all, none of these studies investigated the load-biased behavior of these materials.

While the previous attempts at improving shape memory properties of NiTiPd alloys through solid solution strengthening with boron additions have been unsuccessful [6], more recent work by Bigelow et al [17] indicated that Pt and Au additions were successful in not only increasing the strength of the austenite phase without significantly impacting the detwinning stress, but also significantly increased the dimensional stability of TiNiPd alloys under load-biased thermal cycling, along with increasing the temperature capability of the alloys (See Figure 13). Very minor additions of Hf show even more potential in this regard [11].

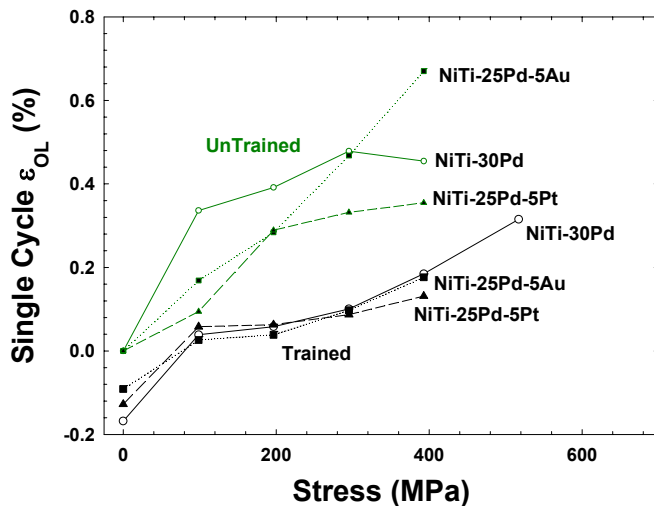


Figure 13: Effect of solid solution strengthening and thermomechanical processing (in this case training) on the amount of ratcheting or open loop strain ( $\epsilon_{OL}$ ) observed.

Precipitate strengthening is another possible route to improving the performance of high temperature shape memory alloys and initial work by Shimizu et al. [7], indicated that the no-load shape memory performance of a NiTiPd alloy was improved considerably by that process. NiTiPt alloys also naturally lend themselves to precipitate strengthening as shown previously by Rios et al. [18] and further work is ongoing in that area.

A final route for improving the properties of shape memory alloys is through thermomechanical processing. Initial efforts in this area have shown that training of TiNiPd alloys, by thermal cycling the material with a bias load in excess of the typical working load for a small number of transformation cycles, reduces the amount of permanent deformation during a load-bias thermal cycle by over 99%, once the material is returned to a lower working bias stress [17]. Also, various combinations of cold work, annealing, and training have been shown to result in a dimensionally stable TiNiPt alloy with long cyclic life, good transformation strain, and enhanced resistance against ratcheting [19]. In both cases, the thermomechanical processing significantly enhanced the resistance of the martensite phase to slip, probably through the development of a stable dislocation network in the material.

Thus, given all the potential options for optimizing and improving the performance of high-temperature shape memory alloys it is quite likely that some engineered versions of these materials will shortly find use in applications up to 300 °C and that within a few years it may be possible to develop alloys with reasonable properties for use in the 400 – 500 °C range.

## Summary

In general, the mere exhibition of shape memory effect does not translate into a material that would be adequate for device applications. Other material characteristics are more important, especially if the intended application involves work against an external load. Of primary importance is the relationship between deformation characteristics of the martensite and austenite phases. In order to achieve a material which exhibits good work characteristics, the austenite phase must have adequate strength, which is significantly greater than the stress required to deform the martensite phase by detwinning. Also, the martensite must have adequate resistance to slip so that the majority of the deformation can be accommodated through the reversible detwinning processes. Finally, the material must also have adequate tensile ductility so that one can take advantage of the strength differences to achieve significant work capability. When all of these factors exist, the material will exhibit good work characteristics (reasonable work output with good dimensional stability).

As such, ternary NiTi-based alloys with Pt and Pd additions show significant promise as high-force shape memory alloys but are limited to transformation temperatures in the range of 100-300 °C. Beyond that temperature range, the work characteristics are poor as a result of the inversion in the relative strengths of the austenite and martensite phases that accompanies the higher alloying levels. However, additional approaches such as solid solution strengthening, thermomechanical processing and/or precipitation strengthening are available to materials designers in order to develop engineered alloys for operation at even higher temperatures.

## Acknowledgements

This work was sponsored by the NASA Fundamental Aeronautics Program – Supersonics Project Office, Propulsion 21, and the NASA Glenn IR&D fund.

## References

- [1] Lindquist, P.G. and Wayman, C.M., “Shape Memory and Transformation Behavior of Martensitic Ti-Pd-Ni and Ti-Pt-Ni Alloys”, in Engineering Aspects of Shape-Memory Alloys, T.W. Duerig, K.N. Melton, D. Stockel and C.M. Wayman, Eds., Butterworth Heinemann, Boston, (1990) 58-68.

- 
- [2] Wu, S.K. and Wayman, C.M., "Martensitic Transformations and the Shape-Memory Effect in  $Ti_{50}Ni_{10}Au_{40}$  and  $Ti_{50}Au_{50}$  Alloys", *Metallography*, 20 (1987) 359.
- [3] Angst, D.R., Thoma, P.E. and Kao, M.Y., "The Effect of Hafnium Content on the Transformation Temperatures of  $Ni_{49}Ti_{51}$ -XHfX Shape-Memory Alloys", *J. Phys IV 5* (1995) C8-747 to C8-752.
- [4] Pu, Z., Tseng, H. and Wu, K., "Martensite Transformation and Shape-Memory Effect of NiTi-Zr High-Temperature Shape-Memory Alloys", *Smart Structures and Materials 1995: Smart Materials*, SPIE Proc. Vol. 2441 (1995) 171.
- [5] Yang, W.S. and Mikkola, D.E., "Ductilization of Ti-Ni-Pd Shape Memory Alloys With Boron Additions," *Scripta Metall. Mater.* **28**, 161-165, 1993.
- [6] Suzuki, Y., Xu, Y., Morito, S., Otsuka, K., Mitose, K., "Effects of boron addition on microstructural and mechanical properties of Ti-Pd-Ni high temperature shape memory alloys," *Mater. Lett.* **36**, 85-94, 1998.
- [7] Shimizu, S., Xu, Y., Okunishi, E., Tanaka, S., Otsuka, K. and Mitose, K., "Improvement of shape memory characteristics by precipitation-hardening of Ti-Pd-Ni alloys," *Mater. Lett.* **34**, 23-29, 1998.
- [8] Goldberg, D., Xu, Y., Murakami, Y., Morito, S., Otsuka, K., Ueki, T. and Horikawa, H., "Improvement of  $Ti_{50}Pd_{30}Ni_{20}$  High Temperature Shape Memory Alloy by Thermomechanical Treatments," *Scripta Metall. Mater.* **30**, 1349-1354, 1994.
- [9] Cai, W., Tanaka, S. and Otsuka, K., "Thermal Characteristics Under Load in a  $Ti_{50.6}Pd_{30}Ni_{19.4}$  Alloy," *Mater. Sci. Forum* **327-328**, 279-282, 2000.
- [10] Noebe, R. *et al.*, "Properties and Potential of Two (Ni,Pt)Ti Alloys for Use as High-Temperature Actuator Materials," *Smart Structures and Materials 2005: Active Materials: Behavior and Mechanics*, SPIE Conf. Proc. Vol. 5761, (2005), pp. 364-375.
- [11] Bigelow, G., "Effects of Palladium Content, Quaternary Alloying, and Thermo-Mechanical Processing on the Behavior of Ni-Ti-Pd Shape-Memory Alloys for Actuator Applications", *Master's Thesis*, Colorado School of Mines, Golden, Colorado, 2006.
- [12] Rasmussen, G. K. *et al.*, "Process for Deposition of Sputtered Shape Memory Alloy Films," U.S. Patent 6,454,913 (2002).
- [13] Zhang, J., "Processing and Characterization of High-Temperature Nickel-Titanium-Hafnium Shape Memory Thin Films," PhD Thesis, Michigan State University, (2002).
- [14] Noebe, R. *et al.*, "Properties of a  $Ni_{19.5}Pd_{30}Ti_{50.5}$  high-temperature shape memory alloy in tension and compression," *Smart Structures and Materials 2006: Active Materials: Behavior and Mechanics*, SPIE Conf. Proc. Vol. 6170, (2006).
- [15] Donkersloot, H.C. and Van Vucht, J.H.N., *J. Less Com. Met.* 20 (1970) 83.
- [16] Biggs, T., Cortie, M.J., Witcomb, M.J. and Cornish, L.A., *Metall. Mater. Trans.* 32A (2001) 1881.
- [17] Bigelow, G., *et al.*, "Development and Characterization of Improved High Temperature Shape Memory Alloys by Solid Solution Strengthening and Thermomechanical Processing of NiTiPd Alloys," SMST 2006 (current conf. proc.), (2006).
- [18] Rios, O. *et al.*, "Characterization of Ternary NiTiPt High-Temperature Shape Memory Alloys," in *Smart Structures and Materials 2005: Active Materials: Behavior and Mechanics*, SPIE Conf. Proc. Vol. 5761, (2005), pp. 376-387.
- [19] Noebe, R., *et al.*, "Effect of Thermomechanical Processing on the Microstructure, Properties, and Work Behavior of a  $Ti_{50.5}Ni_{49.5}Pt_{20}$  High-Temperature Shape Memory Alloy", SMST 2006 (current conf. proc.), (2006).